

Finite-element modeling of hydrothermal circulation in a layered medium adjacent to a cooling magma body

Alan Rice

*Department of Earth and Planetary Sciences, American Museum of Natural History,
79th Street and Central Park West, New York, New York, 10024, USA
and*

*Stony Brook Southampton, State University of New York
239 Montauk Hwy, Southampton, New York, 11968-6700, USA*

ABSTRACT

Computational fluid-dynamics modeling via finite element methods can yield estimates of minimum distances that hydrothermal flow may be mobilized by magmatic heat. As an example, the heat from a chamber 10 km thick embedded in the crust 2 km below Earth's surface can drive horizontal hydrothermal flow more than 100 km within a 1-km-thick zone of rock that is relatively permeable (e.g., 10^{-13} m²) in comparison to the surroundings (e.g., 10^{-15} m²). If the end of the high permeability zone is open, then recharge occurs through tighter rock above and below into the conduit and there is no return flow within the conduit itself. If the end of the conduit abuts an aquaclude, then the return circulation is in the conduit itself, often in the form of a series of porous media convection cells that line the conduit from one end to the other. The geothermal gradient alone is capable of generating convection cells of hydrothermal flow and cannot be neglected because it significantly influences the hydrothermal circulation induced by the magma chamber. Model configurations are similar to the geologic settings of some mineral deposits reported in the literature. Model results support speculations that a number of sources of precious metals are derived from crustal rocks rather than from magmas associated with subduction.

INTRODUCTION

The effort here was initially motivated by the need to investigate the nature of the Witwatersrand gold deposits in South Africa. Our numerical investigations set out to address the physical plausibility of a hydrothermal genesis of the Witwatersrand gold against which had been offered a placer origin. There seems little doubt now that the gold is detrital with later hydrothermal overprints (e.g., Kirk et al., 2002, 2003; Frimmel, 2005). Literature has suggested that magmatic heat might be a driving force of these hydrothermal flows (e.g., Kirk et al., 2003) but does not adequately address the question of physical plausibility. Addressing the issue precipitated useful insights across a wider range of hydrothermal environments and provided insights that are the focus of this paper.

Earlier objections to a hydrothermal origin of the Witwatersrand reef were based on the inference that it was inconceivable that there were any processes of sufficient vigor to cause to a hydrothermal deposition of gold over such large distances as the expanse of the reef. No quantitative assessments seem to have attended these objections although appeal to analytic expressions (e.g., Turcotte and Schubert, 1982) provide back-of-the-envelope estimations which do not prohibit the possibility. Norton and Knight's (1977) numerical modeling of hydrothermal convection by finite differences led them to suggest "The extent of circulation, and magnitude of convective heat flux over broad crustal regions... may be much greater than suspected."

The initial effort here (Rice et al., 1998; Mbandezi et al., 1999) took advantage of finite-element procedures instead,

e-mail: arice@amnh.org

Rice, Alan, 2008, Finite-element modeling of hydrothermal circulation in a layered medium adjacent to a cooling magma body, *in* Spencer, J.E., and Tittley, S.R., eds., *Ores and orogenesis: Circum-Pacific tectonics, geologic evolution, and ore deposits*: Arizona Geological Society Digest 22, p. 127-135.

which are not limited by geometry, allowing more robust assessments as well as yielding more detail. The commercial code ANSYS was employed for the computational work which allowed incorporation of variable viscosity as well as phase change in the magma chamber and allowed coupling the freezing and cooling of the chamber to the attendant ground-water convection. Mathematical and computational background may be found on the ANSYS website: www.ansys.com.

This effort does not treat metasomatic processes which are believed to require longer time frames than initially addressed here (e.g., Rose, 1995). Although the codes employed in this effort are capable of handling multi-phase flow, supercritical fluids, saline solutions and chemistry (such as HCl), these complications, important as they are (e.g., Williams-Jones and Heinrich, 2005), were deferred until other objectives were secured. Likewise, water only from the country rock (meteoric and connate) is treated here; the effect of magmatic water is deferred to a later date as the modeled chambers examined here are sufficiently shallow that permeability could be anticipated in the country rock (e.g., Hedenquist and Shinohara, 1997). SI units are employed throughout. Degrees Kelvin are used as the thermodynamic portions of the codes require it. The magma in all cases is considered granitic and hence has a high initial viscosity. The presentations are restricted to two dimensions. Keeping to simplicity avoids cluttering a clear view of the original target: some indication of the influence of magmatic heat on the volumetric extent of ground-water circulation. A geothermal gradient was also included but is not resolved in the temperature color scale because of the much greater range of temperatures the scale must embrace to depict the cooling history of the magma chamber and hydrothermal system. For graphical representation of both temperature and velocity, red represents the maximum magnitude and blue represents the minimum. Velocities are further characterized by arrows indicating flow direction. Velocity magnitudes are provided only for the ground-water flow (from 10^{-5} m/s to 10^{-13} m/s) as magma convection velocities were in some cases greater than 10^{-1} m/s in the early stages of cooling. Permeability values for granodioritic gneiss, shale and some other rocks are reported to range from 10^{-13} m² to 10^{-15} m² (e.g., Morrow et al., 1994) and these were employed as representative for the initial work. Permeability contrast of two orders of magnitude between actual geological units hosting economic deposits are noted in the literature (e.g., Rowe, 2001; Swensen and Person, 2000); some contrasts are reported for units separated by only half a meter (Shmonov et al., 1997; Sausse et al., 2005). The smaller permeability was assigned to the host rock and the larger employed to simulate fractured or brecciated zones or soft sedimentary rock.

COMPUTATIONAL RESULTS

Homogeneous magma-host rock

We start simply. Figure 1 comprises the first case: a model of an idealized square magma chamber, 1 km vertical

by 1 km horizontal, set in uniformly permeable (10^{-15} m²) country rock. The country rock is bounded by aquacludes top, bottom and sides, encasing the chamber in country rock 3 km by 3 km. Regardless the initial geometry of a freezing magma chamber, model chambers always evolve toward a spherical shape before complete solidification. Any protrusion exhibits enhanced heat transfer into the country rock (like a cooling fin) and quickly solidifies and cools. Figure 1A is the initial temperature distribution, uniform throughout to start. The initial temperature of the magma is set at 1000° K. The lowest temperature accommodated by the color scale is 300° K. The heat of the chamber immediately initiates ground-water circulation up the sides of the chamber. There are two regions of intensity: an outer blue halo of low velocity flow and a tight boundary of intense flow next to the chamber. The velocities given (Figure 1B) are for the ground water, not for the magma which is experiencing turbulent convection. Figures 1C and 1D show the thermal and flow regimes after viscous termination of magma convection. The light blue swell at the bottom of Fig. 1C reflects the influence of the geothermal gradient.

Layered magma-host rock

Figure 2 represents calculations that better address the original objective by introducing a horizontal layer more permeable than the surrounding country rock (10^{-13} m²). Except for attaching a lower permeability to the layer, no other characteristic is assigned to it, but it could represent a fracture zone, sandstone sandwiched between shales, etc. Model circulation in the permeable layer demonstrates that the permeable layer essentially 'short-circuits' the ground-water flow, confining it almost entirely within the permeable layer. Figure 2A displays an oddity in the magma chamber. A crystal laden layer of magma that is still convecting, albeit slower, has descended to the bottom of the chamber, essentially stratifying it. This phenomenon is discussed elsewhere (e.g., Rice, 1998). Note that Fig. 2B, shows the magma chamber to be in the throes of turbulent convection. Figure 2C shows the growth of the temperature perturbation in the country rock due to the ground-water flow in the permeable layer. Figure 2D depicts the shrinking of the magma chamber as it freezes and shows magma circulation only in the molten core of the intrusion. Hydrothermal flow is now fully developed in the permeable layer, outbound at the top of the layer and returning along the bottom. Note further in Figure 2C that the ground-water circulation affects the freezing of the magma chamber, giving isotherms in the crystallized magma a 'waist' where it abuts the permeable layer. The hot ground-water circulation in the permeable layer also has greatly distorted the temperature distribution in the country rock from the uniform permeability situation shown in Figure 1C. Figure 2E shows the continued development of the distorted temperature field due to circulating ground water even after the magmat-convection termination. Residual heat maintains the ground water circulation as indicated in Figure 2F. Some mild circulation

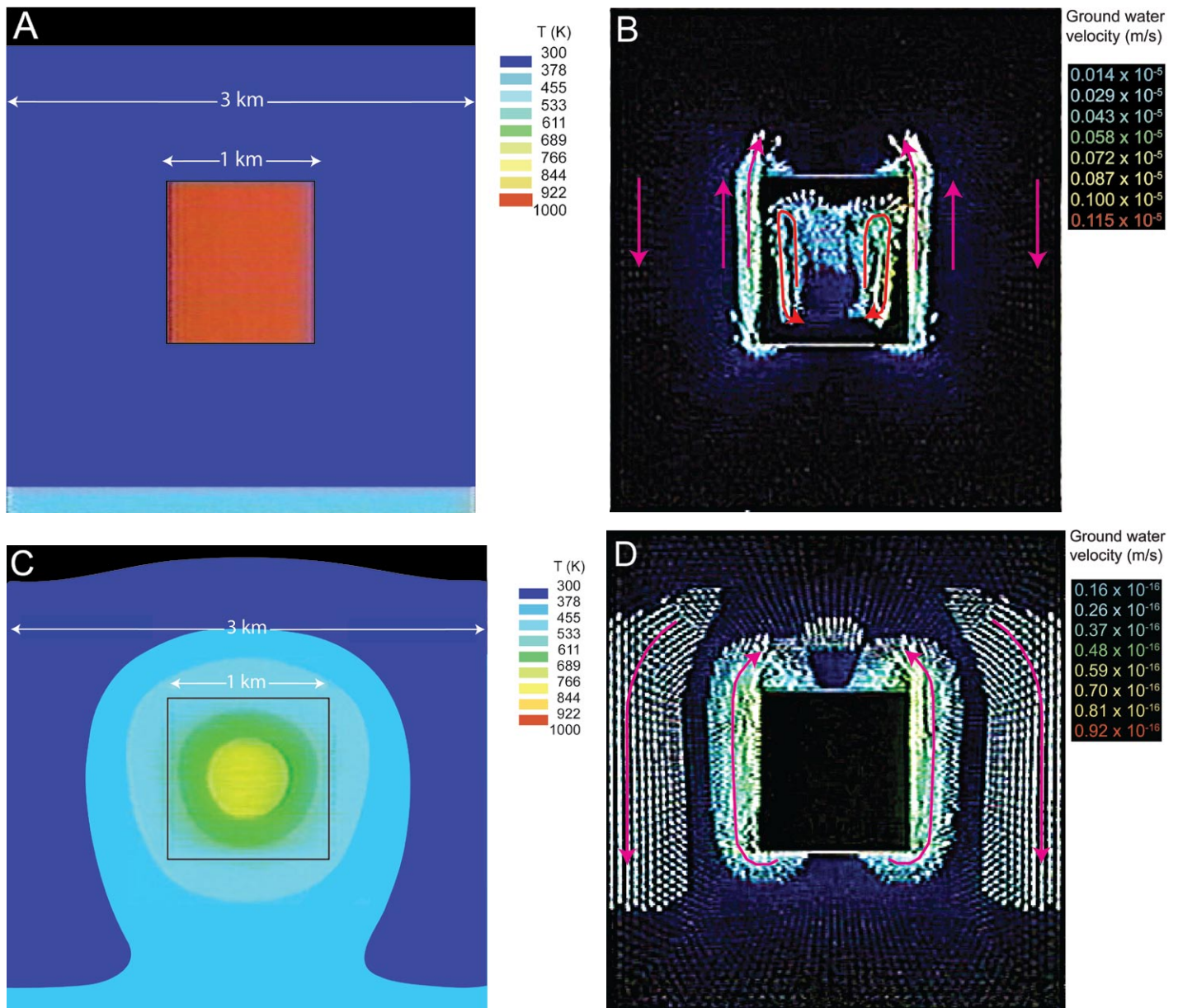


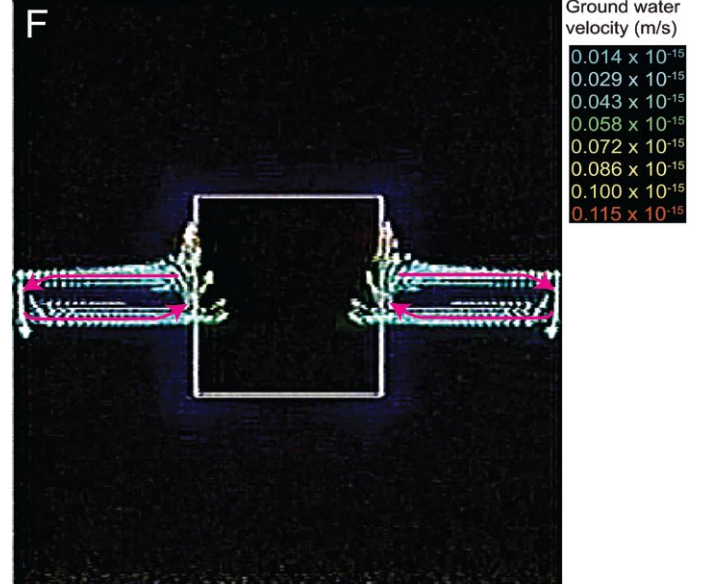
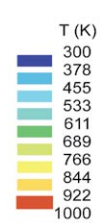
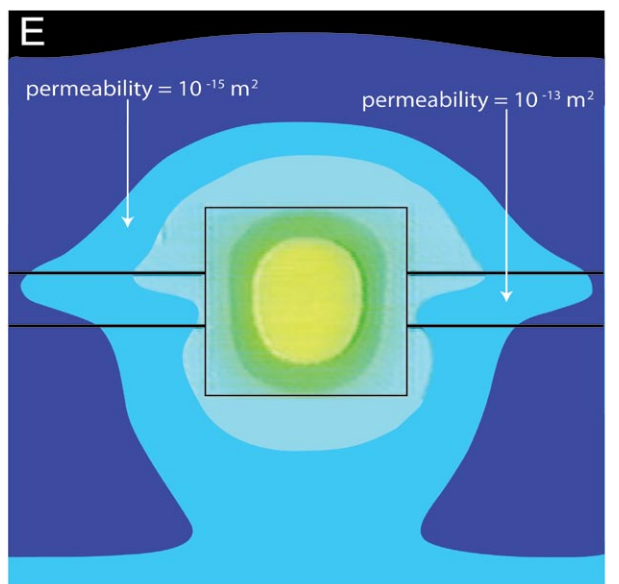
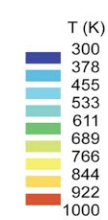
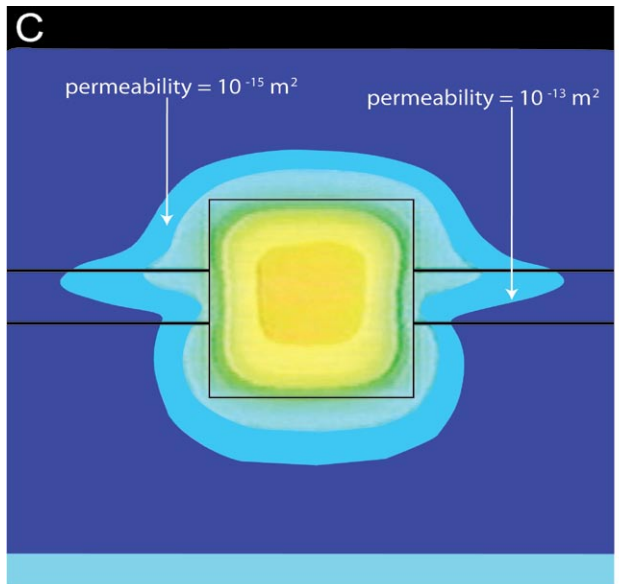
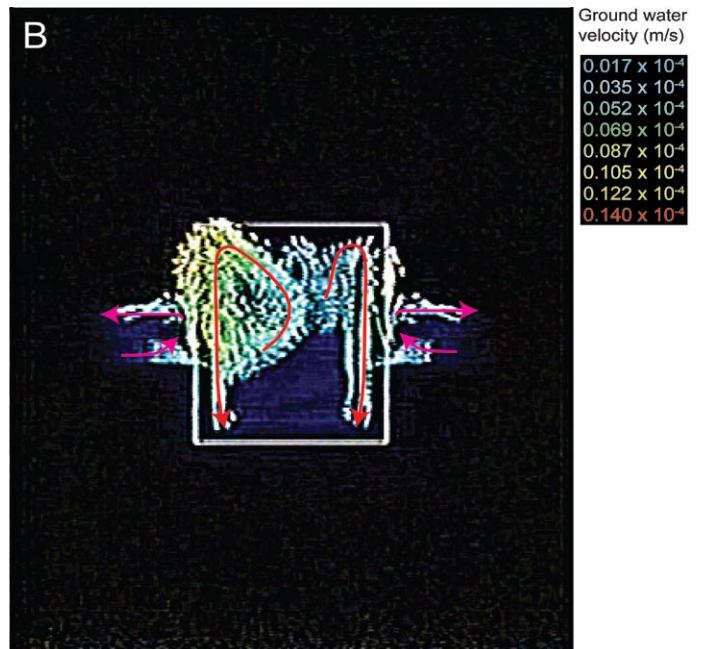
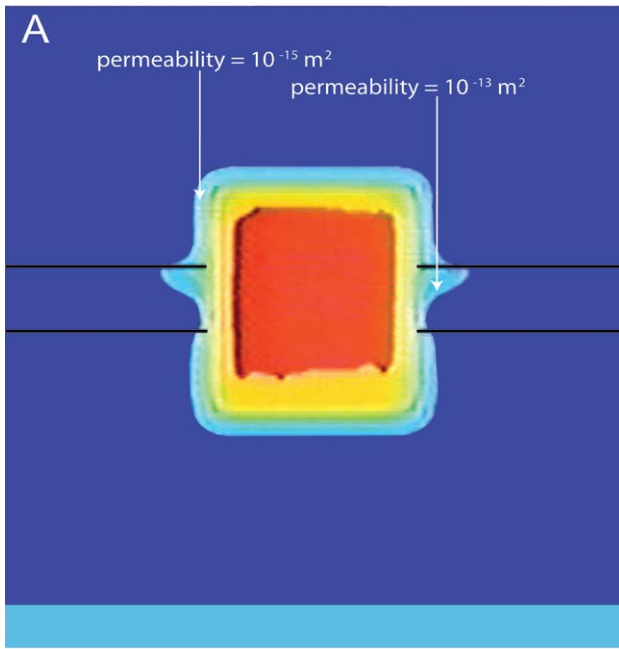
Figure 1. Two-dimensional numerical simulation of temperature and fluid movement following instantaneous emplacement of a 1 km (horizontal) x 1 km (vertical) magma body into a homogeneous medium. (A) Initial temperature. (B) Early convective hydrothermal fluid circulation. Flow vectors produced by the numerical simulation are not clearly visible due to limitations with graphics capabilities of the computer graphics hardware used here, but are approximated by the superimposed red and magenta arrows. Red arrows represent magma flow, magenta arrows represent hydrothermal-fluid flow. (C) Temperature profile shortly after viscous termination of magma convection (~5000 years after magma emplacement), and (D) associated hydrothermal flow in host rocks.

surrounds the nearly frozen chamber as indicated by the faint blue halo around it. The warm section at the bottom of Figure 2E reflects the influence of the geothermal gradient. Note that as the chamber cools and solidifies, the intensity (velocity) of the hydrothermal circulation falls off as well.

Influence of an ambient geothermal gradient

Incorporating more complexities, it is useful to ascertain whether or not the geothermal gradient imposes a circulation

of its own. A simple configuration was employed solely to test the possibility and not to model a specific portion of the Earth's crust. Again, a permeability of 10^{-15} m^2 is employed throughout. Figures 3A and 3B both represent the velocity field, Figure 3A depicting flow direction and Figure 3B depicting velocity magnitude. The boundary and initial conditions were as follows: an imposed geothermal gradient (30° C/km), 20° C on the upper surface boundary, no heat flow through the sides, and no fluid flow across any boundary. A single convection cell is formed with a broad, slightly meandering, central



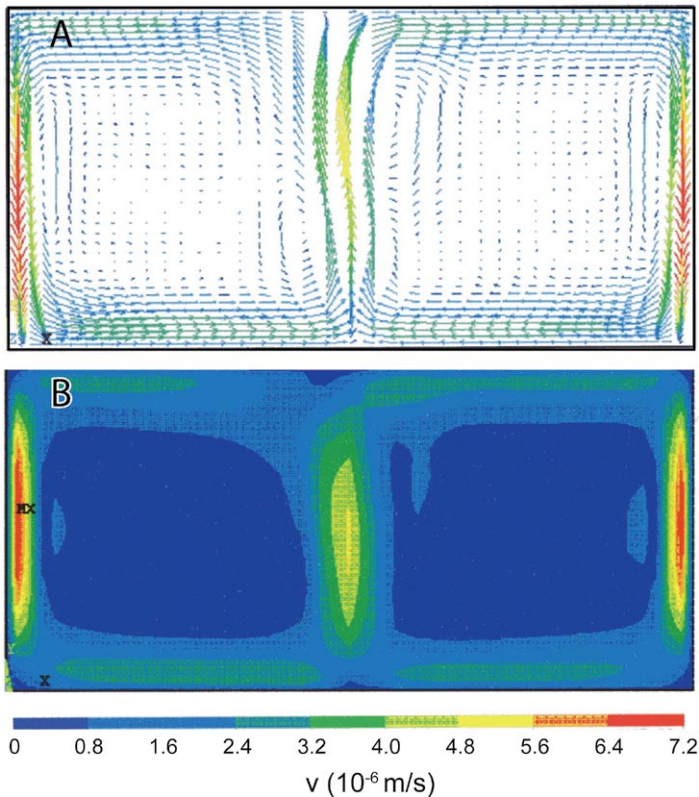


Figure 3 (above). Two-dimensional numerical simulation of hydrothermal fluid flow in a permeable medium caused only by an ambient geothermal gradient of $30^{\circ}\text{C}/\text{km}$. Area modeled is 5 km (vertical) \times 10 km (horizontal).

upwelling, and the circulation is completed along the sides as tight, downward directed flow of greater intensity. The single cell is confined by the closed side boundaries; this is an artificial imposition that can always be relieved in further calculations and which may reveal more complex patterns.

A variety of possible flow fields may result from nearly identical boundary conditions, the particular flow field determined by some small perturbation in the starting conditions.

Figure 2 (facing page). Two-dimensional numerical simulation of temperature and fluid movement following instantaneous emplacement of a one km (vertical) by one km (horizontal) magma body into a layered medium. The horizontal, high permeability layer is between the two dark lines in A, C, and E. Flow vectors produced by the numerical simulation are not clearly visible in B, D, and E, due to limitations with graphics capabilities of the computer hardware used here. These flow vectors are approximated by the superimposed red and magenta arrows. Red arrows represent magma flow, magenta arrows represent hydrothermal fluid flow. (A) Temperature profile and (B) convective magma and hydrothermal-fluid circulation shortly after magma emplacement. (C) Temperature profile and (D) fluid circulation shortly before complete crystallization of the magma (at ~ 1600 model years). (E) Temperature profile and (F) hydrothermal fluid circulation following magma crystallization (at ~ 2700 model years).

Atmospheric flow patterns are an example: broad upwellings and narrow downwellings or vice versa can obtain under the same circumstances.

Regardless of the simplicity of the model, it is clear that an ambient geothermal gradient is capable of generating circulation without additional heat from a magma chamber. The model configuration, with dimensions of 5 km by 10 km, allows hydrothermal circulation. If the layer were only a kilometer deep, however, Rayleigh numbers for permeable media flow suggest that the geothermal gradient could not mobilize convection.

Layered magma-host rock with an ambient geothermal gradient

The geothermal gradient will also influence flow that is driven by magmatic heat from a magma chamber emplaced in the crust. Figure 4 displays hydrothermal flow in a permeable (relative to the country rock), 100-m-thick, horizontal conduit, driven by both the magmatic heat and heat from below (the geothermal gradient). A square magma chamber is again employed and is displayed as 'red hot'. The chamber is 1 km by 1 km and the dimensions of the region of interest are 5 km deep by 10 km horizontal. Boundary conditions are the same except that flow is allowed across all boundaries. Because the aquifer is then open at the far end to the left as well, there is no return flow within the conduit. The fluid is taken to be incompressible; continuity requirements (conservation of mass) then require recharge from the country rock. This is manifest in the right corner of Figure 4A with the upwelling of warm water from below. Again, as the fluid is incompressible, cold ground water is pushed ahead as warm water is supplied behind it at the face of the magma chamber. This is obvious from Fig. 4A which displays an initial lack of any warm water in the conduit although fluid is already mobilized down the conduit as seen in Fig 4E. Figures 4B and 4C display the evolution of the temperature in the surrounding country rock as warm water rises from below to make up for the flow that exits on the left side. The warm-water flow is developed at this time and is clearly visible in the conduit in Figure 4B and faintly visible in Figure 4C as underlying warm water (due to the geothermal gradient) has been driven upward to replace fluid that is leaving out the left side. Computer runs without the geothermal gradient did not show this effect: there was no warm water to rise from below.

It is emphasized that recharge is from the country rock, and this occurs along the entire length of the more permeable conduit. The magma chamber, while molten, was modeled as impermeable in these calculations. Hence, the magma not only blocks recharge in its vicinity but more importantly, its own heat drives away or keeps away rising warm fluid from the depths immediately below the chamber (Figs. 4C, D). This is because the pore pressure around the chamber is higher due to the thermal expansion of pore water surrounding the chamber, creating a pore pressure gradient that suppresses

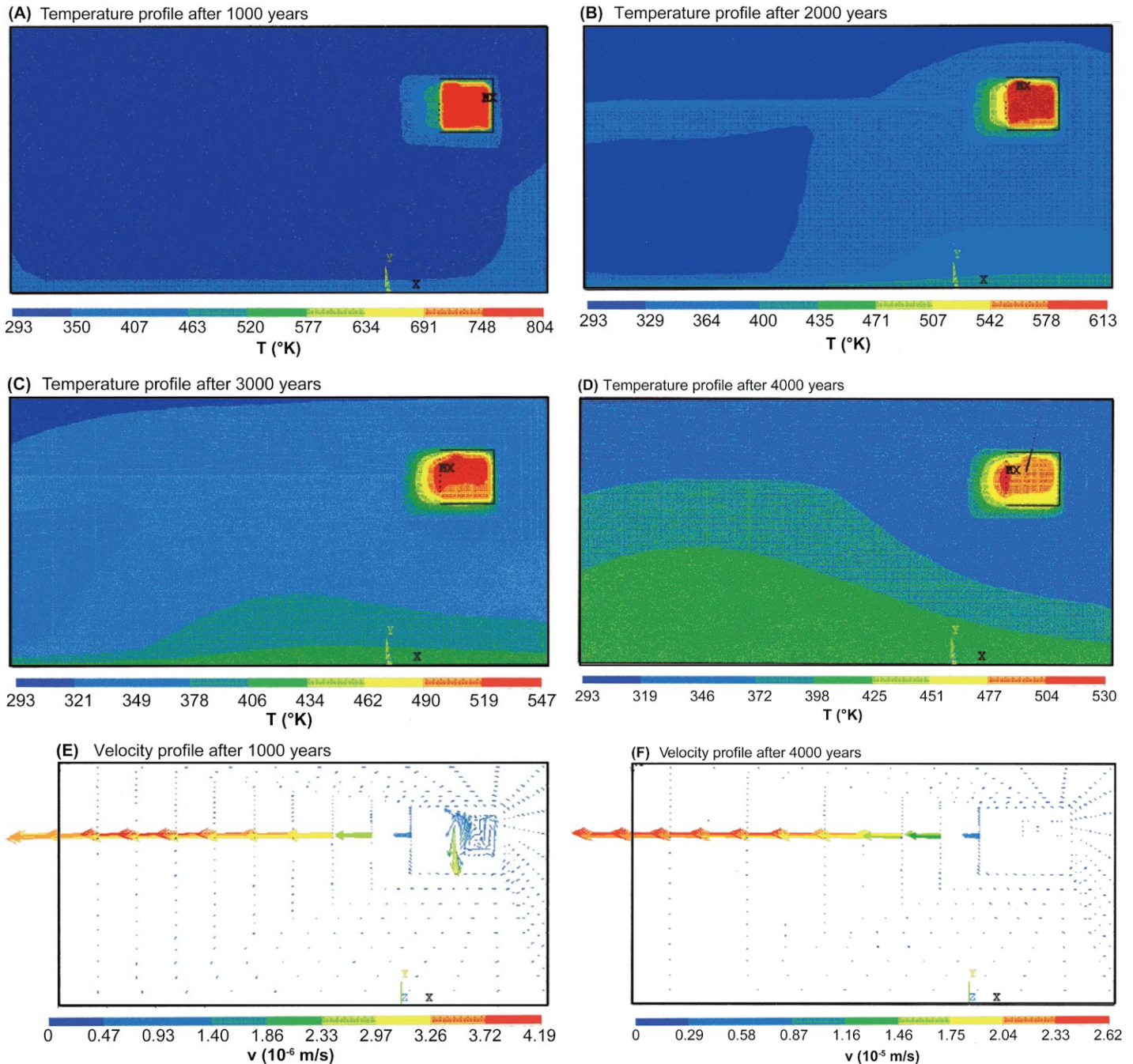


Figure 4. Two-dimensional numerical simulation of temperature and fluid movement following instantaneous emplacement of a 1 x 1 km magma body into a layered medium. The model area is 5 km (vertical) x 10 km (horizontal). The horizontal, high-permeability layer is 100 m thick and extends to the left from the magma body. See text for boundary conditions. Temperature profiles are shown in Figures A, B, C, and D; Fluid-flow vectors corresponding to A and D are shown in E and F. Note that values for color scales are different for each figure.

ground-water flow toward the chamber. Although initiating beneath the chamber, the recharge from the underlying rocks is forced by the heat of the magma chamber to skirt around the chamber and to move to the left, rising away from the impediment posed by the chamber itself. If the sides were closed, and the chamber symmetrically oriented, this option would not be available. Figures 4D and 4F demonstrate that, although the mobilized ground water flow from below is becoming a domi-

nant feature within the country rock, the flow in the country rock itself, with permeability 2 orders of magnitude less than that of the conduit, is barely manifest in the velocity profiles shown in Figure 4F. The velocity of the flow in the conduit, driven by heat from the magma chamber, is far greater.

After 4000 model years, the heated region surrounding the magma chamber is warm enough and has expanded enough to be easily seen in the color contrasts employed to

depict the temperature field in Figure 4D. It is in this heated region that thermal expansion of pore water has created a pore pressure gradient, pushing ground water away from the chamber and forcing recharge of the conduit from further afield, bringing up fluids from deeper, underlying warmer sections of the crust.

Figure 5 displays the time evolution that attends a much wider (500 m) conduit. The profiles are similar to those of the 100-m-thick conduit discussed above. There are differences, but they are not profound. One item to note is that the flow is tighter across the top of the chamber; presumably because the more intense flow in the 500-m conduit (which offers less resistance than the 100-m conduit) has pulled in the boundary layer across the top of the chamber. Note that the wider conduit accommodates faster flow. In all cases, the flows eventually slow as the chamber cools. Further, these flows are not impeded by a return flow within the permeable zone itself.

The original objective was eventually addressed: Is a hydrothermal system as large as the Witwatersrand reef possible? Computer runs were made of models similar to those above in Figures 4 and 5. However, the model magma chamber was 5 km by 5 km and the permeable layer one km thick and extending 100 km from the source of heat. The end was open. The results showed that there would be no difficulty of hosting a hydrothermal system of this extent in the crust, and it was likely that larger systems would be manifest.

Three-dimensional models were also run, but discussion of these results is deferred to another paper. It is to be noted, however, that in three dimensions, ground-water flow is not always symmetric about the magma chamber and with time meanders around the chamber, intense first on one side and then intense on another.

IMPLICATIONS, SPECULATIONS, AND CONCLUSION

Modelling hydrothermal convection in a medium of constant permeability surrounding a magma chamber suggests that the hydrothermal fluids rising alongside the chamber are confined to a thin plume next to the magma chamber. Mineralization at the highly brecciated Cripple Creek gold deposit is similarly distributed - that is, tight against the chamber wall (Vardiman et al., 2008). Unless the magma intrudes layers of variable permeability (e.g., fracture zones or layered sedimentary rocks), the “virtual” model above (Fig. 1) compares well with Figures 14.5, 14.6, and 14.7 in Evans (1993) that depict scenarios similar to the Lowell and Gilbert (1970) “light bulb” model for porphyry copper genesis. From other considerations, the eventual penetration of ground water into the magma chamber would likely occur initially in the outer several hundred meters (measured from the wall inward). The reason for this is that the chill zone next to the wall rock will experience the greatest thermal stress since initially the greatest temperature difference occurs there. The center of the chamber loses heat more slowly and is characterized by

lower thermal gradients (there is no horizontal gradient at all at the center). The high thermal gradients during cooling of the intrusion margins, and associated fracturing due to thermal-related stresses, would be expected to produce a shell of fractures and, if fluids are metal laden, mineralized rock, as with porphyry copper deposits.

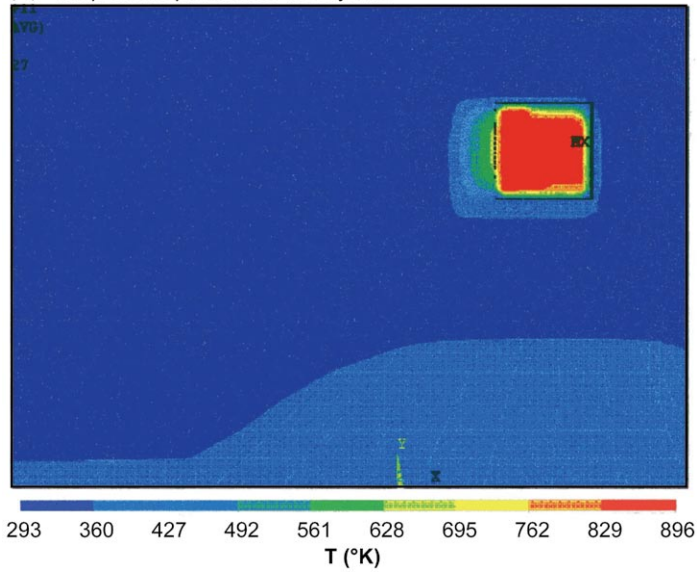
A numerical simulation presented here indicates that an ambient geothermal gradient can cause hydrothermal circulation without imposition of a magma chamber. If a magma chamber is emplaced in the crust, the combined effect of both the geothermal gradient and the chamber appears to mobilize massive hydrothermal circulation that will sweep through and sample large volumes of crustal rock. Such a process would provide physical support for Tittley’s (1987) suggestion that “precious metal characteristics may represent inheritance from specific kinds of crust rather than derived from partial melts associated with subduction” (see also Mathur et al., 2000). It is also to be noted that hydrothermal circulation develops essentially instantaneously, lending support to assertions of geologically rapid ore-deposit genesis, such as the following from Heinrich (2006): “The enormous hydrothermal gold ore deposit on Lihir Island, Papua Guinea, may have formed in less than 55,000 years.”

The permeable layer models might well be an idealized but approximate representation of the original geological environment of the Massif Central deposits ((Bouchot et al., 2005), or the Pogo Mine in Alaska (Johnson, 1999; Rombach et al., 2002) where there is a granitic batholith apparently related to the deposit but about 1.5 km distant.

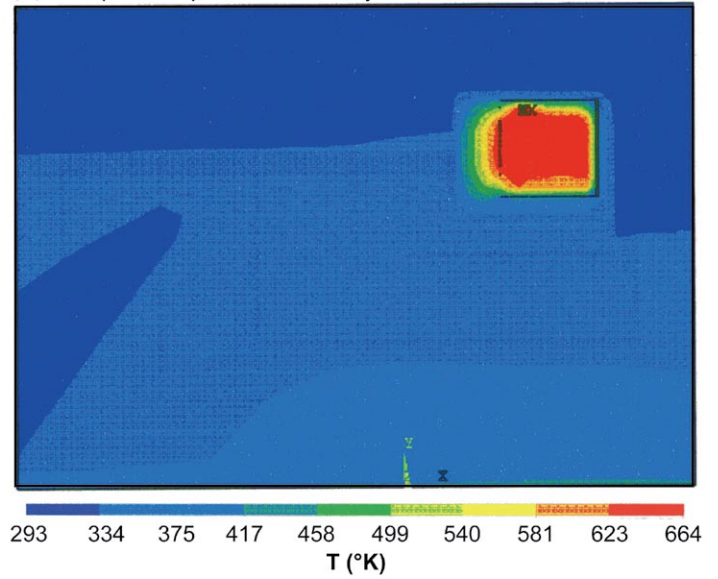
Permeable layers do not outcrop in the models. Mineralization produced by hydrothermal circulation in a confined, sub-horizontal layer will not outcrop unless exhumed by erosion or tectonics. Economic mineralization has yet to be associated with the plutons of Cape Granite suite of South Africa. These plutons intrude the Precambrian Malmesbury Supergroup sedimentary rocks which rarely outcrop; consequently the stratigraphy of the Malmesbury Supergroup is poorly known (Belcher and Kisters, 2003) but conceivably could host mineralization related to circulation like that modelled here. This modeling supports the speculations of Johnson (1999) which may be applicable to the Cape Granite suite:

“Although outcropping mineralization continues to be discovered in some parts of the world, it is widely accepted that new discoveries in many areas will require exploration for deep targets. Deep mineralization may be concealed by unmineralized bedrock and/or post-mineral cover. Two examples of recent discoveries...are...the large San Nicolas polymetallic volcanogenic massive sulfide deposit in central Mexico and the high-grade gold deposit at Pogo in east-central Alaska. Neither discovery involved the simple application of a conventional ore deposit model in well-understood areas. Both required a combination of careful geological observations and interpretation, pragmatic exploration techniques, and a flexible approach”.

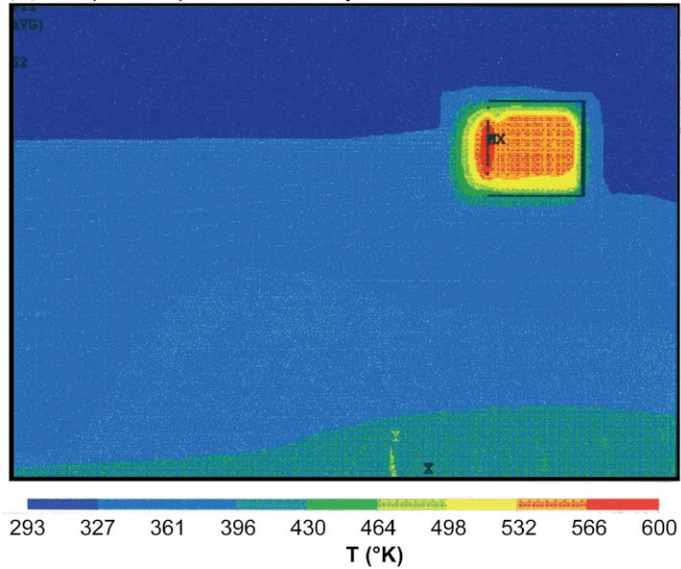
(A) Temperature profile after 1000 years



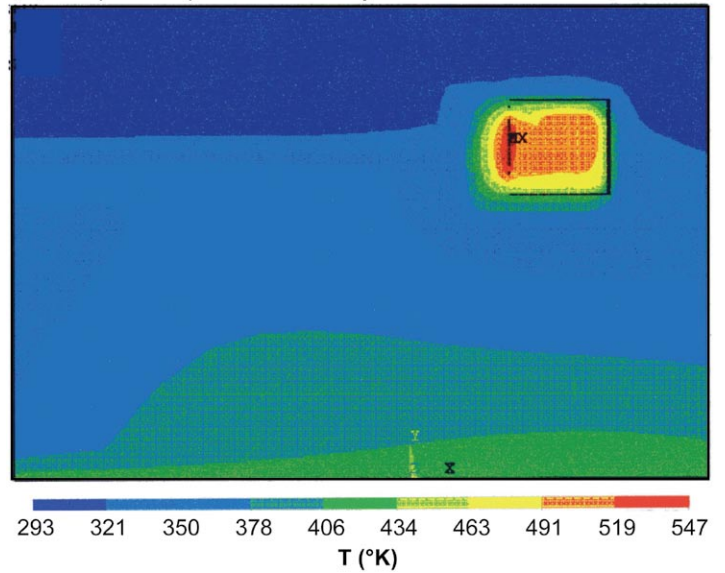
(B) Temperature profile after 2000 years



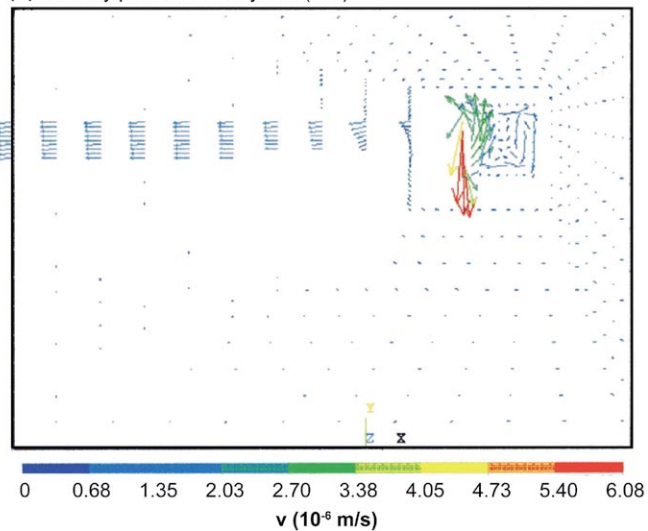
(C) Temperature profile after 3000 years



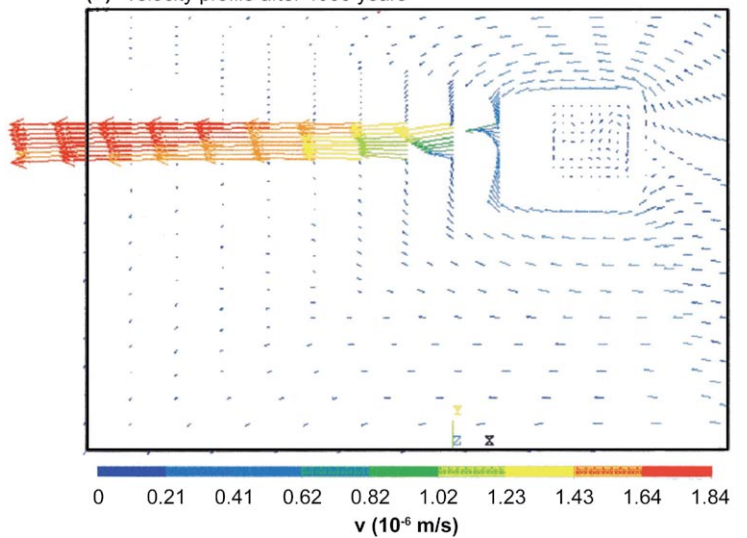
(D) Temperature profile after 4000 years



(E) Velocity profile at 1000 years (m/s)



(F) Velocity profile after 4000 years



Computational fluid dynamics should be added to this tool box. It certainly seems to have bearing on the issue of the source of precious metals, whether from partial melts derived from subduction or scavenged from crustal rocks by extensive hydrothermal convection fields. For the moment, this modeling favors the latter of these two possibilities.

ACKNOWLEDGMENTS

I am indebted to Spencer Titley for his kind elucidation of certain aspects of the Lowell-Gilbert models, and to Jon Spencer and Sarah Jane Fowler for editorial assistance.

REFERENCES CITED

- Belcher, R.W. and Kisters, A.F.M., 2003. Lithostratigraphic correlations in the western branch of the Pan-African Saldania belt, South Africa: The Malmesbury Group revisited: *South African Journal of Geology*, v. 106, p. 327-342.
- Bouchot, V., Ledru, P., Lerouge, C., Lescuyer, J.-L., and Milesi, J.-P., 2005. Late Variscan mineralizing systems related to orogenic processes: The French Massif Central: *Ore Geology Reviews*, v. 27, p. 169-197.
- Evans, A.M., 1993. *Ore Geology and Industrial Minerals: An Introduction*: Oxford, U.K., Blackwell Science, 3rd Edition, 400 p.
- Frimmel, H.E., 2005. Archaean atmospheric evolution: Evidence from the Witwatersrand gold fields, South Africa: *Earth Science Reviews*, v. 70, p. 1-46.
- Hedenquist, J.W., and Shinohara, H., 1997. K-silicate- to sericite-stage transition in porphyry Cu deposits: Collapse of magmatic plume, or overprint by meteoric water? [abs.]: *Geological Society of America Abstracts with Programs*, v. 28, p. A-402.
- Heinrich, C., 2006. How fast does gold trickle out of volcanoes?: *Science*, v. 314, p. 263-264.
- Johnson, J.F.H., 1999. Discovery of new deposits at depth: Examples of a flexible approach to exploration: Sydney Mineral Exploration Discussion Group, Exploring Under Cover, Symposium, North Sydney, Australia, Sept. 24, 1999, accessed 2008 at <http://www.smedg.org.au/Sym99Keynote.htm>
- Kirk, J., Ruiz, J., Chesley, J., Walshe, J., England, G., 2002. A major Archean, gold- and crust-forming event in the Kaapvaal Craton, South Africa: *Science*, v. 297, p. 1856-1858.
- Kirk, J., Ruiz, J., Chesley, J., and Titley, S., 2003. The origin of gold in South Africa: *American Scientist*, v. 91, p. 534-541.
- Lowell, J.D., and Gilbert, J.M., 1970. Lateral and vertical alteration-mineralization zoning in porphyry ore deposits: *Economic Geology*, v. 65, p. 373-408.
- Mathur, R., Ruiz, J., Titley, S., Gibbins, S. and Margotomo, W., 2000. Different crustal sources for Au-rich and Au-poor ores of the Grasberg Cu-Au porphyry deposit: *Earth and Planetary Science Letters*, v. 183, p. 7-14.
- Mbandezi, L., Remsing, C., and Rice, A., 1999. The importance of structure in hydrothermal mineralization: Finite element analyses of fluid flow mobilized by magmatic intrusions [abs.]: *EOS, Transactions of the American Geophysical Union*, v. 80, p. F1099.
- Morrow, C., Lockner, D., Hickman, S., Rusanov, M., and Rockel, T., 1994. Effects of lithology and depth on the permeability of core samples from the Kola and KTB drill holes: *Journal of Geophysical Research*, v. 99, p. 7263-7274.
- Norton, D., and Knight, J.E., 1977. Transport phenomena in hydrothermal systems: Cooling plutons: *American Journal of Science*, v. 277, n. 8, p. 937-981.
- Rice, A., Botha, A., Harrison, K., Moore, J.M., Bangay, S., Clayton, P., and Panagou, S., 1998. 3-Dimensional calculations of transport processes associated with convection in freezing magma chambers and attendant hydrothermal circulation: some preliminary implications for ore body formation: *South African Conference on Applied Mechanics '98*, Cape Town, South Africa, Jan. 12-14, 1998, p. 1177-1180.
- Rice, A., 1998. Toward computer modelling of ore body formation by a multi-disciplinary approach: some initial results pertaining to the cooling of buried bodies of molten rock (magma chambers) and attendant hydrothermal circulation: *South African Journal of Science*, v. 94, p. 53-57.
- Rombach, C.S., Newberry, R.J., Goldfarb, R.J. and Smith, M., 2002. Geochronology and mineralization of the Liese zones, Pogo Deposit, Alaska [abs.]: *Geological Society of America Annual Meeting, Denver, Colorado, October 27-30, 2002, Final Program*, accessed 2008 at http://gsa.confex.com/gsa/2002AM/finalprogram/abstract_45183.htm
- Rose, N.M., 1995. Geochemical consequences of fluid flow in porous basaltic crust containing permeability contrasts: *Geochimica et Cosmochimica Acta*, v. 59, n. 21, p. 4381-4392.
- Rowe, R.K., ed., 2001. *Geotechnical and Geoenvironmental Engineering Handbook*: Norwell, Massachusetts, Kluwer Academic Publishers, 1160 p.
- Sausse, J., Fourar, M., and Genter, A., 2005. Petrophysics and Permeability in the Soultz Granite: *World Geothermal Congress 2005, Antalya, Turkey, April 24-29, 2005, Proceedings*, p. 1-6.
- Shmonov, V.M., Lakshtanov, D.L. and Borisov, M.V., 1997. Permeability of wallrocks of the hydrothermal vein Pb-Zn ore mineralization, in *Experiment in Geosciences: Journal of the Institute of Experimental Mineralogy (IEM) (Russian Federation)*, v. 5, article 18.
- Swensen, J.B. and Person, M., 2000. The role of basin-scale transgression and sediment compaction in stratiform copper mineralization: implications from White Pine, Michigan, USA: *Journal of Geochemical Exploration*, v. 69-70, p. 239-243.
- Titley, S.R., 1987. The crustal heritage of silver and gold ratios in Arizona ores: *Geological Society of America Bulletin*, v. 99, p. 814-826.
- Turcotte, D.L. and Schubert, G., 1982. *Geodynamics: Applications of Continuum Physics to Geological Problems*: New York, John Wiley and Sons, 450 p.
- Vardiman, D.M., Brown, T.R., Roy, E., Ward, M., and Hutchinson, I.P., 2008. *Geology of the Cripple Creek mining district: Cripple Creek and Victor Gold Mining Co.*, accessed 2008 at <http://www.ccvgoldmining.com/Geology/geology.html>
- Willaims-Jones, A.E. and Heinrich, C.A., 2005. Vapor transport of metals and the formation of magmatic-hydrothermal ore deposits: *Economic Geology*, v. 100, n. 7, p. 1287-1312.

Figure 5 (facing page). Two-dimensional numerical simulation of temperature and fluid movement following instantaneous emplacement of a 1 x 1 km magma body into a layered medium. The model area is 5 x 10 km. The horizontal, high-permeability layer is 500 m thick and extends to the left from the magma body. See text for boundary conditions. Temperature profiles are shown in Figures A, B, C, and D; Fluid flow vectors corresponding to A and D are shown in E and F. Note that values for color scales are different for each figure.

